11th World Congress on Computational Mechanics (WCCM XI)
5th European Conference on Computational Mechanics (ECCM V)
6th European Conference on Computational Fluid Dynamics (ECFD VI)
E. Oñate, J. Oliver and A. Huerta (Eds)

NUMERICAL SIMULATION OF UNSTEADY WIND-INDUCED CONDUCTOR OSCILLATIONS

OLGA A. IVANOVA*

* Applied Mathematics Department
Bauman Moscow State Technical University
2-nd Baumanskaya st., 5, 105005 Moscow, Russia
e-mail: ivanovaolgaal@mail.ru

Key words: Mathematical Modeling, Transmission Line, Galloping, Vortex Element, Viscous Vortex Domains Method, Parallel Algorithm, MPI Technology

Abstract. The mathematical model of aeroelastic motion of the transmission line conductor is considered. Parallel program for the conductor motion simulation is developed. The unsteady aerodynamic loads on the conductor cross-sections were calculated using viscous vortex domains method. Some test computations were performed. The results of the computations were compared to known experimental and numerical data.

1 INTRODUCTION

An overhead transmission line conductor which is covered by an asymmetric icing can be subjected to galloping — high-amplitude low-frequency oscillations caused by the stable cross-wind. High dynamic loads during galloping can lead to significant damage of the line and its hardware, therefore the problem of numerical and experimental modeling of the conductor dynamics is of theoretical and practical importance [1].

The important part of the conductor dynamics simulation is the aerodynamic loads computation. The flat cross-section method is usually adopted, i.e. the flow around each conductor cross-section is assumed to be plane-parallel and the aerodynamic load in the direction of the conductor axis is neglected. Moreover, the aerodynamic loads are usually assumed to be quasi-steady. It hasn't been investigated yet if this assumption is always adequate. Though in many cases the agreement between numerical and experimental results is good [2, 3], it is not clear how the real unsteadiness of the aerodynamic forces influences the conductor motion. But as the conductor has a large spatial extent, the full three-dimensional numerical simulation of its aeroelastic interaction with wind is hardly possible.

In this research the simplified approach to the direct numerical simulation of the unsteady aeroelastic conductor motion is proposed. The flat cross-section method is used

and the unsteady aerodynamic loads in N separate conductor cross-sections are calculated using meshfree lagrangian viscous vortex domains method [4]. Thus a three-dimensional problem is replaced by a set of N partially independent two-dimensional problems of the flow simulation around the conductor cross-sections. The computer program based on the proposed algorithm is developed. In order to reduce the computational time parallel implementation of the most time-consuming stages of the algorithm is performed using MPI technology.

2 GOVERNING EQUATIONS

2.1 Governing equations for the conductor dynamics

Let us locate the Cartesian coordinate system so that the transmission line in the equilibrium position without aerodynamic loads is located in the plane Ox_1x_3 (fig. 1).

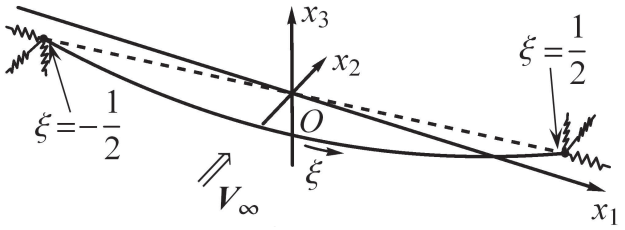

Figure 1: The design diagram

The conductor is considered to be absolutely flexible and linearly elastic. The system of its motion equations is based on the equations [5] which are supplemented by the terms caused by the conductor cross-sections eccentricity and by the equation for the twist angle:

$$\left(\frac{Q}{1+Q/EF}x_1'\right)' + C_1 - \ddot{x}_1 = 0, \tag{1}$$

$$\left(\frac{Q}{1+Q/EF}x_2'\right)' + C_2 + \left(1+\frac{Q}{EF}\right)q_2^a - \ddot{x}_2 - h\left(\sin(\theta_s+\theta)\ddot{\theta} + \cos(\theta_s+\theta)\dot{\theta}^2\right) = 0, \tag{2}$$

$$\left(\frac{Q}{1+Q/EF}x_3'\right)' + C_3 + \left(1+\frac{Q}{EF}\right)q_3^a - 1 - \ddot{x}_3 - h\left(\cos(\theta_s+\theta)\ddot{\theta} - \sin(\theta_s+\theta)\dot{\theta}^2\right) = 0, \tag{3}$$

$$(x_1')^2 + (x_2')^2 + (x_3')^2 = \left(1+\frac{Q}{EF}\right)^2, \tag{4}$$

$$GJ\theta'' + C_\theta + M^a - \ddot{\theta} - h\beta\Big(\sin(\theta_s+\theta)\ddot{x}_2 + \cos(\theta_s+\theta)\ddot{x}_3 + \cos(\theta_s+\theta)\Big) = 0. \tag{5}$$

Here dimensionless parameters are: $\xi \in [-0.5, 0.5]$ — natural coordinate on the unstretched conductor, τ — time; $Q(\xi,\tau)$ — tension; $x_i(\xi,\tau)$, $i = 1,2,3$ — cartesian coordi-

nates of the conductor axis; $\theta(\xi,\tau)$ — twist angle of the conductor; $C_i(\xi,\tau)$, $C_\theta(\xi,\tau)$ — the functions describing the internal damping forces; $q_k^a(\xi,\tau)$, $k=2,3$, $M^a(\xi,\tau)$ — the aerodynamic loads; $EF=\text{const}$ — axial stiffness; GJ — torsional stiffness; $\theta_s(\xi)=\theta_e(\xi)+\theta_G$, $\theta_e(\xi)$ — rotation angle of the unloaded conductor cross-sections; β — parameter characterizing the conductor inertia. The conductor cross-sections are assumed to be orthogonal to its axis, the axis position in the cross-section is point C. The center of gravity G of the iced conductor cross-section is specified with the distance $h=CG$ and the angle θ_G which is measured at the position corresponding to zero angle of incidence as shown on fig. 2. The derivatives with respect to ξ and τ are denoted by prime and dot respectively. The units of length, mass and force are the unstretched conductor length $\tilde{L}$, mass and weight respectively; the unit of time is $\sqrt{\tilde{L}/\tilde{g}}$ where $\tilde{g}$ is dimensional gravity acceleration.

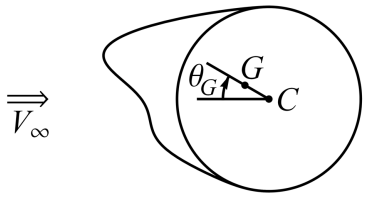

Figure 2: The center of gravity of the conductor cross-section

Initial condition is the equilibrium position in the gravity field $x_{i0}(\xi)$, $i=1,2,3$, $Q_0(\xi)$, $\theta_0(\xi)$.

At the ends $\xi=\pm1/2$ the conductor is fixed by the linear static springs which simulate the insulator strings and the adjacent spans

$$\begin{gathered} x_i(\pm1/2,\tau)-x_{i0}(\pm1/2)=S_i^{\pm}\left(Q\boldsymbol{p}^{\pm}-Q_0\boldsymbol{p}_0^{\pm}\right)\Big|_{\xi=\pm1/2}\cdot\boldsymbol{e}_i,\quad i=1,2,3,\\ \theta(\pm1/2,\tau)=0. \end{gathered} \tag{6}$$

Here $\boldsymbol{p}^{\pm}$, $\boldsymbol{p}_0^{\pm}$ are unit vectors tangential to the conductor axis at time moments τ and τ_0 respectively (fig. 3); $S_i^{\pm}$, $i=1,2,3$, are the compliances of the linear static springs which model the adjacent spans and the insulator strings.

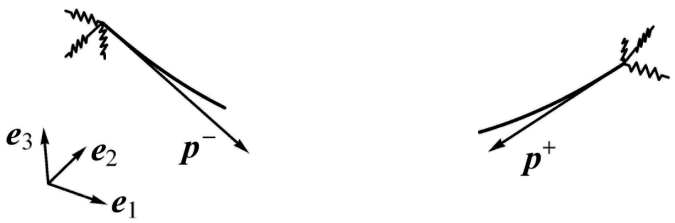

Figure 3: Unit vectors tangential to the conductor axis

2.2 Governing equations for the flow dynamics

The flow around all conductor cross-sections is assumed to be plane-parallel so that all the characteristics of the flow don't depend on the x_1 coordinate. The viscous incompressible flow around the airfoil (conductor cross-section) is described by continuity equation

$$\nabla \cdot \boldsymbol{V} = 0$$

and Navier — Stokes equation

$$\frac{\partial \boldsymbol{V}}{\partial t} - \boldsymbol{V} \times \boldsymbol{\Omega} = -\nabla \left(p + \frac{V^2}{2} \right) + \frac{1}{\mathrm{Re}} \nabla^2 \boldsymbol{V},$$

where dimensionless parameters are: $\boldsymbol{V}(x_2, x_3, t)$ — fluid velocity, $\boldsymbol{\Omega} = \nabla \times \boldsymbol{V} = \Omega \boldsymbol{e}_1$ ($\boldsymbol{e}_1$ is axis Ox_1 unit vector) — vorticity, $p(x_2, x_3, t)$ — pressure, Re — Reynolds number. Boundary condition on the airfoil contour is no-slip condition; on infinity all perturbations decay and the flow has uniform velocity $\boldsymbol{V}_\infty$ and pressure p_∞. The aerodynamic loads acting on the airfoil can be determined via the pressure distribution $p(x_2, x_3, t)$.

3 NUMERICAL METHODS

3.1 Solution of the governing equations

The conductor motion equations are solved using Galerkin method according to which the conductor coordinates and tension are taken in the form

$$x_i(\xi, \tau) = x_{i0}(\xi) + \sum_{k=1}^{n_i} a_k^{(i)}(\tau) \varphi_k^{(i)}(\xi), \quad i = 1, 2, 3,$$

$$\theta(\xi, \tau) = \theta_0(\xi) + \sum_{k=1}^{n_\theta} a_k^{(\theta)}(\tau) \varphi_k^{(\theta)}(\xi), \quad Q(\xi, \tau) = Q_0(\xi) + \sum_{k=1}^{n_Q} a_k^{(Q)}(\tau) \varphi_k^{(Q)}(\xi).$$

The basis functions for the coordinates $\varphi_k^{(i)}(\xi)$ are the eigenmodes of the conductor small free oscillations (assuming additionally that $h = 0$) which are computed by the accelerated convergence method [6] and two extra functions needed to correctly satisfy the nonlinear boundary conditions (6); the same procedure is used to choose the basis functions $\varphi_k^{(Q)}(\xi)$. To simplify the numerical simulation algorithm the systems of basis functions are orthogonalized. The basis functions for the twist angle θ are trigonometric: $\varphi_k^{(\theta)}(\xi) = \sqrt{2} \sin \pi k(\xi + 1/2)$. The orthogonality condition of the equations (1)–(5) residual to the basis functions allows to obtain the system of $(n_1 + n_2 + n_3 + n_\theta - 6)$ ordinary differential and $(n_Q + 6)$ algebraic equations in the unknown functions $a_k^{(*)}(\tau)$.

The functions $C_j(\xi, \tau)$, $j = 1, 2, 3$, $C_\theta(\xi, \tau)$ which describe the internal damping forces are taken in the form

$$C_j(\xi, \tau) = -2\zeta_j \sum_{k=1}^{n_j - 2} \omega_k^{(j)} \frac{da_k^{(j)}(\tau)}{d\tau} \varphi_k^{(j)}(\xi), \qquad C_\theta(\xi, \tau) = -2\zeta_\theta \sum_{k=1}^{n_\theta} \omega_k^{(\theta)} \frac{da_k^{(\theta)}(\tau)}{d\tau} \varphi_k^{(\theta)}(\xi),$$

where ω_k are the eigenfrequencies of the conductor small free oscillations; ζ_j, ζ_θ are the damping coefficients.

The flow around each cross-section of the conductor is simulated using meshfree lagrangian viscous vortex domains method [4] with the modified numerical scheme [7]. This method has the following advantages:

- it allows to calculate the aerodynamic loads acting on the arbitrary airfoil with adequate accuracy in acceptable time;
- the simulations of the flow around stationary and moving airfoils require almost the same computational time;
- the modified numerical schemes using the tangential velocity components on airfoil surface allow to considerably reduce the oscillatiopns of the aerodynamic loads;
- it allows to develop effective parallel implementation [8].

3.2 The algorithm of unsteady conductor motion simulation

The following parallel computer algorithm based on MPI technology usage is proposed to simulate the unsteady aeroelastic conductor motion. The unsteady aerodynamic loads are calculated at N equally-spaced conductor cross-sections; the flow around each cross-section is simulated by a group of m processors. Each group has a local main processor (LMP); the main processor of the first group is also the main processor (MP) of the whole task. At each time step the following operations are executed.

1. Each group solves two-dimensional problem of the flow around one cross-section during 1 time step (fig. 4).
2. LMP's calculate the aerodynamic loads on the cross-sections and send calculated values to MP.
3. MP interpolates aerodynamic loads acting on the cross-sections to obtain $q_2^a(\xi,\tau)$, $q_3^a(\xi,\tau)$, $M^a(\xi,\tau)$ and solves the nonlinear system obtained via Galerkin method during 1 time step.
4. MP broadcasts coefficients $a_k^{(i)}$, $a_k^{(\theta)}$, $a_k^{(Q)}$ and their time derivatives to all processes.
5. All processes calculate the positions and angles of the cross-sections on the next time step.

On the base of the proposed algorithm the parallel computer program PROVOD is developed. It allows also to perform quasi-steady computation, i.e. to use the stationary aerodynamic drag C_{xa}, lift C_{ya} and moment C_m coefficients of the cross-sections instead of simulation of the flow around them. The program PROVOD can as well be used to

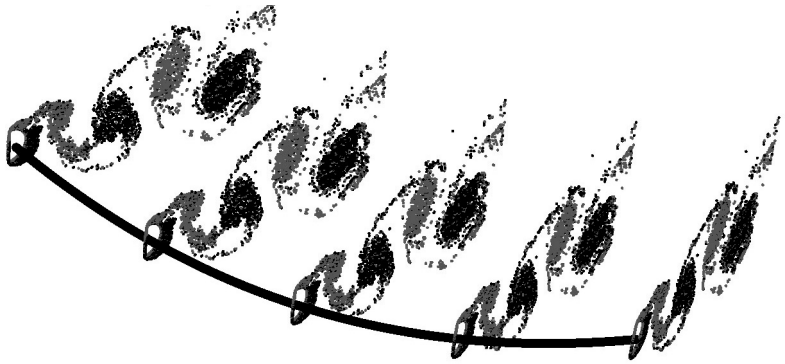

Figure 4: Flat cross-section method llustration

calculate the stationary aerodynamic coefficients for different angles of incidence α. In addition it can be used to simalate the unsteady wind-induced motion of single airfoil with elastic constraints.

The development of periodic high-amplitude galloping motion sometimes takes considerable time (hundreds of seconds). To reduce the time of computation it is proposed to execute quasi-steady simulation until the periodic trajectory is reached and then to change the way of the loads calculation and to execute the unsteady simulation using viscous vortex domains method.

4 NUMERICAL EXAMPLES

4.1 Quasi-steady simulation

The galloping motion observed for the central span of the three-span test line is described in [9]. The central span was covered by an artificial U-shaped "icing" (fig. 5). This case of galloping was reproduced numerically in [2, 10] assuming that the aerodynamic loads were quasi-steady.

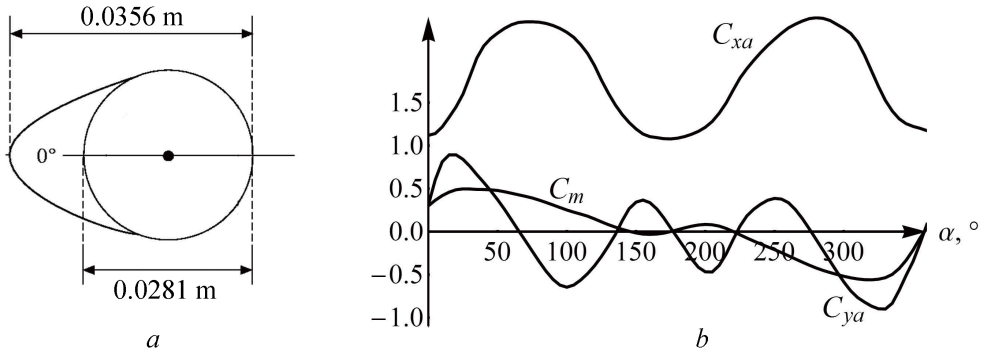

Figure 5: U-shaped cross-section [9] (a) and its stationary aerodynamic coefficients [10] (b)

The analysis of the stationary aerodynamic coefficients shows that Den-Hartog aerodynamic instability condition [11]

$$C_{xa}(\alpha) + C'_{ya}(\alpha) < 0$$

is satisfied for the angles of incidence $\alpha \in [17°; 90°]$, $\alpha \in [152°; 204°]$, $\alpha \in [261°; 327°]$.

Dimensional parameters of the line (as given in [2, 12]) are shown in Table 1.

Table 1: Transmission line parameters

Parameter	Notation	Unit	Value
Span length	$\tilde{L}$	m	243.8
Axial stiffness	$\widetilde{EF}$	10^6 N	29.7
Torsional stiffness	$\widetilde{GJ}$	N·m^2/rad	300
Horizontal component of tension	$\tilde{Q}_0(0)$	10^3 N	32.0
Bare conductor diameter	$\tilde{d}$	10^{-3} m	28.1
Damping coefficients	ζ_1=ζ_2=ζ_3	10^{-2}	0.44
Damping coefficient	ζ_θ	10^{-2}	1.42
Conductor mass per unit length	$\tilde{\rho}$	kg/m	1.8
Inertia moment per unit length	$\tilde{I}$	10^{-4} kg·m	1.69
Distance CG	$\tilde{h}$	m	0.00159
Angle θ_G	θ_G	°	0

The wind velocity is 9 m/s; adjacent spans have the same characteristics as the central span without icing. Insulator strings have length 2 m and mass 38.9 kg.

Dimensionless parameters are the following: axial stiffness $EF = 6909$, torsional stiffness $GJ = 742.5$, $h = 6.5 \cdot 10^{-6}$, $\beta = 6.3 \cdot 10^8$, horizontal component of tension $Q_0(0) = 7.44$, sag-to-span ratio $w = 0.0168$.

The initial rotation angle was $\theta_e = 141°$, so under the action of the gravity force the central cross-section equilibrium orientation angle becomes

$$\theta_s(0) = \theta_e + \theta_0(0) \approx 180°$$

which lies in the instability region predicted by the Den-Hartog condition.

The dimensionless strings' compliances $S_1^{\pm}$, $S_2^{\pm}$ were chosen so that the first eigenfrequencies of the central span with elastically fixed ends were equal to the corresponding eigenfrequencies of the full three-span line (0.29 Hz in the Ox_1x_3-plane and 0.24 Hz in the Ox_2 direction): $S_1^{\pm} \approx 0.00073$, $S_2^{\pm} \approx 0.0095$.

Numerical simulation of galloping of the central span has shown that peak-to-peak amplitude of vertical motion was about 2.3 m. Vertical and angular displacements of the central point of the span from its equilibrium position are shown on fig. 6. The results of this research are in good agreement with the results of numerical simulation [2] and in satisfactory agreement with experiment [9].

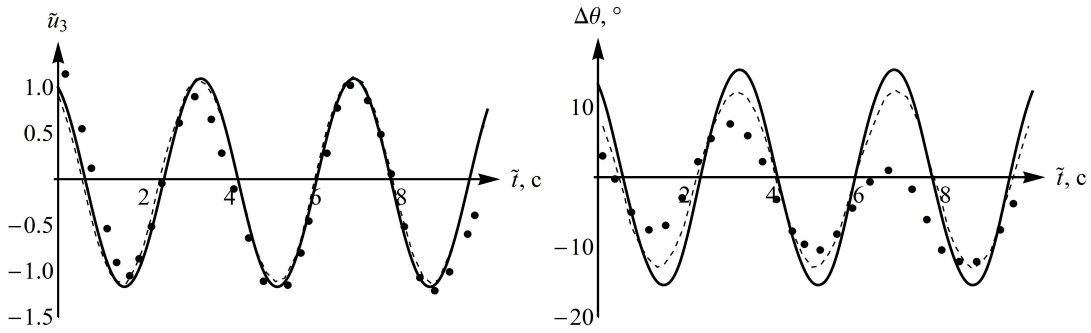

Figure 6: Vertical $\tilde{u}_3$ and angular $\Delta\theta$ displacements of the central point of the span versus time: points — experiment [9], dashed line — simulation [2], solid line — this research

One eigenmode of small free conductor oscillations in each direction was used in the simulation. Test computations show that the increment of the number of basis functions doesn't lead to the perceptible change of galloping characteristics.

4.2 Stationary aerodynamic coefficients calculation

The flow around the iced conductor cross-section shown in [13, 14] was simulated (fig. 7, a). The simulation parameters were the following: vortex element radius $\varepsilon = 0.008$, collapse radius $\varepsilon_{col} = 0.002$, incoming flow velocity $V_\infty = 1$, time step $\Delta\tau = 0.004$, Reynolds number $\mathrm{Re} = 1000$. The airfoil was modeled by 245 panels.

The stationary aerodynamic coefficients C_{xa}, C_{ya}, C_m of the considered airfoil were obtained via time averaging of the corresponding unsteady coefficients over 7 000 time steps. The simulation was performed for the angles of incidence α in the interval from $-40°$ to $50°$ with the step $4°$. The analysis of the dependencies $C_{xa}(\alpha)$, $C_{ya}(\alpha)$, $C_m(\alpha)$ approximated by smooth curves shows that the Den-Hartog instability condition is satisfied in the interval $\alpha \in [-7°; 11°]$.

This airfoil and its stationary aerodynamic coefficients will be used further during the simulation of the conductor galloping.

4.3 Unsteady conductor motion simulation

The unsteady motion of the conductor with the cross-section considered in Section 4.2 is simulated using the algorithm proposed in Section 3.2.

The dimensionless axial rigidity was $EF = 6906$; dimensionless horizontal component of tension $Q_0(0) = 7.44$; the initial cross-section orientation angle was $\theta_e = -46°$ which

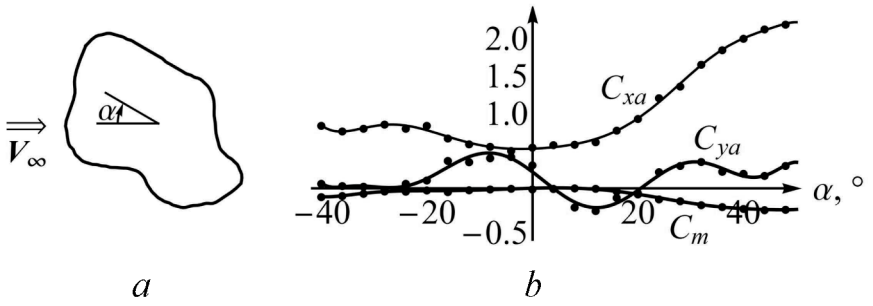

Figure 7: Stationary aerodynamic coefficients $C_{xa}(\alpha)$, $C_{ya}(\alpha)$, $C_m(\alpha)$ of the iced cross-section (a) approximated by smooth functions (b)

under the action of the gravity force results in the central cross-section equilibrium orientation angle close to 7°. The end springs compliances are $S_1^{\pm} = 0.00096$, $S_2^{\pm} = 0.0085$. The basis contains one eigenmode of small free oscillations in each direction.

At first stage the quasi-steady loads were used in the computation until time moment $\tilde{t}^* = 180$ s; on the next stage this computation was continued and the unsteady loads on the conductor cross-sections were determined using viscous vortex domains method. The number of conductor cross-sections considered was equal to $N = 16$; the flow around each of them was simulated in the parallel mode by $m = 8$ processors. Hereby the unsteady calculation required the usage of 128 computing cores of the cluster MVS-100K (Joint Supercomputer Center of the Russian Academy of Sciences) and took about 140 hours. The acceleration of the parallel computation in comparison with the computation in sequential mode was close to 65 times.

Vertical coordinate $\tilde{x}_3(0)$ and angular position $\theta(0)$ of the central point of the span are shown on fig. 8. It can be observed that the galloping amplitude obtained in the unsteady simulation is 12 % less in comparison with the quasi-steady simulation and is finally about 0.65 m. The amplitude of rotational oscillations doesn't change significantly and is approximately 9°. It can be noticed that the conductor natural high-frequency rotational oscillations are superimposed on the rotational motion coherent with the vertical one.

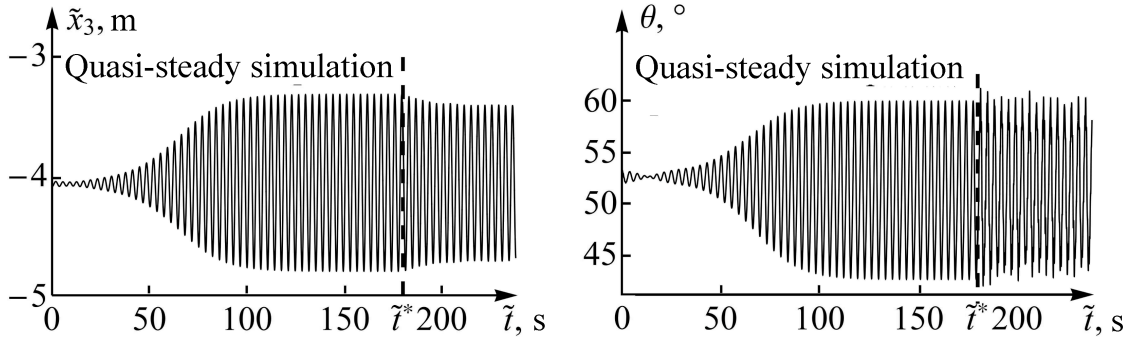

Figure 8: Vertical coordinate $\tilde{x}_3$ and rotation angle θ of the central point on the conductor versus time

5 CONCLUSION

The algorithm of simulation of the aeroelastic oscillations of transmission line conductor with asymmetrical cross-section is proposed. On the base of this algorithm the parallel computer program PROVOD is developed. To simulate the flow around conductor cross-sections and to calculate the unsteady aerodynamic loads acting on them meshfree viscous vortex domains method is used. The program allows also to determine stationary aerodynamic coefficients of the airfoil and to perform quasi-steady simulations. The results of test computations agree well with known experimental and numerical results. The developed algorithm and program can be used to investigate aeroelastic oscillations of extensive constructions under essentially unsteady conditions.

ACKNOWLEDGEMENTS

The work was supported by Russian Federation President Grant for young scientists [proj. MK-3705.2014.8]. The author thanks Joint Supercomputer Center of the Russian Academy of Sciences for the given possibility of supercomputer MVS-100k usage.

REFERENCES

[1] EPRI. *Transmission line reference book: wind-induced conductor motion*. Palo Alto (California): Electrical Power Research Institute (1979).

[2] Keutgen, R. *Galloping phenomena: a finite element approach: Ph.D. Thesis*. Liege (Belgium) (1998).

[3] Waris, M.B., Ishihara, T. and Sarwar, M.W. Galloping response prediction of ice-accreted transmission lines. *The 4th International Conference on Advances in Wind and Structures: book of proceedings*. Jeju (Korea), (2008): 876–885.

[4] Dynnikova, G.Ya. The Viscous Vortex Domains (VVD) method for non-stationary viscous incompressible flow simulation. *The IV European Conference on Computational Mechanics: book of proceedings*. Paris (France), (2010).

[5] Svetlicky, V.A. *Dynamics of rods*. Springer (2005).

[6] Akulenko, L.D. and Nesterov, S.V. *High-precision methods in eigenvalue problems and their applications*. Boca Raton: CRC Press (2004).

[7] Marchevsky, I.K. and Moreva, V.S. Vortex element method for 2D flow simulation with tangent velocity components on airfoil surface. *ECCOMAS 2012, e-Book Full Papers* (2012): 5952–5965.

[8] Moreva, V.S. and Marchevsky, I.K. High-efficiency POLARA program for airfoil aerodynamic characteristics calculation using vortex elements method. *The 5th In-*

ternational Conference on Vortex Flows and Vortex Models: book of proceedings. Caserta (Italy), (2010).

[9] Chan, J.K. *Modelling of single conductor galloping. Canadian Electrical Association Report 321-T-672A*. Montreal (1992).

[10] Desai, Y.M., Yu, P., Shah, A.H. and Popplewell, N. Perturbation-based finite element analyses of transmission line galloping. *Journal of Sound and Vibration*. (1996) **191(4)**: 469–489.

[11] Den Hartog, J. P. Transmission line vibration due to sleet. *AIEE Transactions*. (1932) **51(4)**: 1074–1086.

[12] Wang, X. and Lou, W.-J. Numerical approach to galloping of conductor. *The 7th Asia-Pacific Conference on Wind Engineering: book of proceedings*. Taipei (Taiwan), (2009).

[13] Lukjanova, V.N. *The development of the methods of analysis of absolutely flexible rods (conductors) during icing and unsteady oscillations. Ph.D. Thesis*. Moscow (Russia) (1987). [in Russian]

[14] Marchevsky, I.K. *Mathematical modeling of the flow around an airfoil and its Lyapunov stability investigation: Ph.D. Thesis*. Moscow (Russia) (2008). [in Russian]